AIP | Applied Physics Letters

Effect of “symmetry mismatch” on the domain structure of rhombohedral BiFeO3 thin films

Z. H. Chen, A. R. Damodaran, R. Xu, S. Lee, and L. W. Martin

Citation: Applied Physics Letters **104**, 182908 (2014); doi: 10.1063/1.4875801
View online: http://dx.doi.org/10.1063/1.4875801
View Table of Contents: http://scitation.aip.org/content/aip/journal/apl/104/18?ver=pdfcov
Published by the AIP Publishing

APPLIED PHYSICS LETTERS **104**, 182908 (2014)

Effect of "symmetry mismatch" on the domain structure of rhombohedral $BiFeO_3$ thin films

Z. H. Chen,[1] A. R. Damodaran,[1] R. Xu,[1] S. Lee,[1] and L. W. Martin[1,2,a)]
[1]*Department of Materials Science and Engineering and Materials Research Laboratory, University of Illinois, Urbana-Champaign, Urbana, Illinois 61801, USA*
[2]*Department of Materials Science and Engineering, University of California, Berkeley, Berkeley, California 94720, USA*

(Received 18 March 2014; accepted 28 April 2014; published online 8 May 2014)

Considerable work has focused on the use of epitaxial strain to engineer domain structures in ferroic materials. Here, we revisit the observed reduction of domain variants in rhombohedral $BiFeO_3$ films on rare-earth scandate substrates. Prior work has attributed the reduction of domain variants to anisotropic in-plane strain, but our findings suggest that the monoclinic distortion of the substrate, resulting from oxygen octahedral rotation, is the driving force for variant selection. We study epitaxial $BiFeO_3$/$DyScO_3$ $(110)_O$ heterostructures with and without ultrathin, cubic $SrTiO_3$ buffer layers as a means to isolate the effect of "symmetry mismatch" on the domain formation. Two-variant stripe domains are observed in films grown directly on $DyScO_3$, while four-variant domains are observed in films grown on $SrTiO_3$-buffered $DyScO_3$ when the buffer layer is >2 nm thick. This work provides insights into the role of the substrate—beyond just lattice mismatch—in manipulating and controlling domain structure evolution in materials. © *2014 AIP Publishing LLC*.
[http://dx.doi.org/10.1063/1.4875801]

Ferroic materials (e.g., ferroelectrics, ferromagnets, ferroelastics) typically form domains upon cooling from high temperatures in order to minimize the total free energy of the system.[1] Controlling and understanding such domain formation is of critical importance to the advancement of both fundamental studies and applications of these materials as the configuration of domains is key in determining the ultimate properties of the material.[2,3] In this regard, it is well known that the domain structure of ferroic materials is generally sensitive to the thermal, field, elastic, etc., forces applied to the material. In turn, considerable effort has focused on the use of epitaxial thin-film strain as a way to manipulate, deterministically, the elastic boundary conditions and gain control of the domain structure of materials.[2–4] Most studies of epitaxial thin-film strain have focused on the simple concept of lattice mismatch (i.e., the sign and magnitude of epitaxial strain),[4] while the effect of "symmetry mismatch" (i.e., arising from a difference in crystal symmetry; particularly, in perovskites where a large variety of octahedral rotations and distortions can produce a range of crystal symmetries derived from a cubic parent structure)[5] between film and substrate has received considerably less attention.

Such concerns become increasingly important when one studies the epitaxy of a film and substrate possessing different symmetries (e.g., cubic and rhombohedral). For instance, studies of rhombohedral ferroic materials, including ferromagnets, such as $La_{0.7}Sr_{0.3}MnO_3$[6,7] and the multiferroic $BiFeO_3$,[8–11] have revealed four- and two-variant domain structures for films grown on cubic, (001)-oriented and orthorhombic, $(110)_O$-oriented substrates, respectively. (Note that we will use cubic or pseudocubic indices throughout this Letter unless otherwise specified and that the subscript "*O*" denotes orthorhombic indices.) Focusing now on $BiFeO_3$ as a prototypical rhombohedral ferroic material, in the bulk, $BiFeO_3$ possesses a rhombohedrally distorted perovskite structure with a pseudocubic lattice parameter $a = 3.965$Å, $\alpha = 89.4°$, and space group $R3c$.[12] This, in turn, allows for an $a^-a^-a^-$ antiphase oxygen octahedral rotation (noted in Glazer notation)[13] to occur in this material. In thin-film form, the rhombohedral symmetry is reduced due to the in-plane biaxial strain, resulting in a monoclinic lattice with polarization along $\langle 111 \rangle$.[14] Subsequently, there are a total of four energetically degenerate structural variants (i.e., elastic domains variants) [Fig. 1(a)], each of which can possess two possible polarization variants,[15] which can give rise to potentially complicated domain patterns with up to eight possible domain variants.[16] In materials such as $BiFeO_3$, not only the domain structures play a role in the ferroelectric properties[17] but also the domain walls themselves can possess exotic properties such as electronic conduction.[18] Thus, gaining control over the formation of domain structures is imperative to the ultimate function of the material.

This, in turn, has driven numerous studies that have demonstrated deterministic control over the evolution of domain structure[8–10,19] and the hypothesis that anisotropic in-plane lattice parameters of orthorhombic substrates can give rise to selection of a sub-set of the domain variants.[7,9,19] These observations, however, are surprising considering that the strain anisotropy from such orthorhombic substrates is quite small, for instance, the misfit strains between $BiFeO_3$ and $DyScO_3$ $(110)_O$ are -0.3% and -0.4% along the $[001]_O$ and $[1\bar{1}0]_O$, respectively. Such small differences in the magnitude of the anisotropic in-plane strain make it difficult to explain the striking difference in domain variant selection occurring in films grown on cubic and orthorhombic substrates.[10,11] In fact, prior theoretical calculations have suggested that such a small anisotropy in the in-plane strain cannot explain a broken degeneracy between the eight

---

[a)] Electronic mail: lwmartin@berkeley.edu

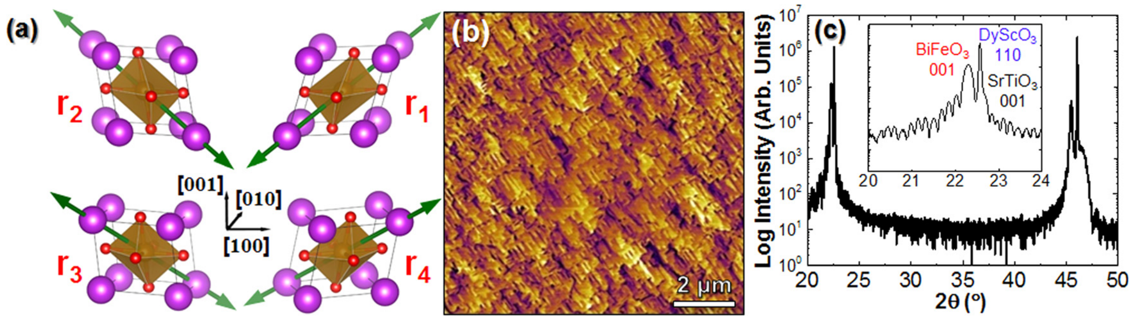

FIG. 1. (a) Illustrations of all four structural variants in rhombohedral BiFeO$_3$ where the arrows represent the directions of the spontaneous polarization. A typical (b) AFM topographic image and (c) XRD $\theta - 2\theta$ scan of a 50-nm-thick BiFeO$_3$ film grown on 10 nm SrTiO$_3$-buffered DyScO$_3$ $(110)_O$ substrate. Inset shows the enlarged region around 001-diffraction condition of BiFeO$_3$.

polarization variants observed in thin films.[20] Therefore, besides lattice mismatch between the substrate and film, other factors, such as symmetry mismatch, also need to be carefully taken into account to explain the wide-spread observations of domain variant reduction.

In this work, we use the model rhombohedral ferroic material BiFeO$_3$ grown on orthorhombic DyScO$_3$ $(110)_O$ substrates with and without ultrathin, buffer layers of the cubic material SrTiO$_3$ to directly probe the role of symmetry mismatch, rather than just lattice mismatch, in determining the domain variant selection in rhombohedral ferroic films. To accomplish this, a series of ultrathin, fully strained SrTiO$_3$ buffer layers with thicknesses ranging from 0–10 nm were grown on DyScO$_3$ substrates prior to the BiFeO$_3$ growth, thereby producing a series of samples with the same in-plane lattice mismatch, but with varying symmetry mismatch. Subsequently, two-variant stripe domain structures were observed in films grown directly on the DyScO$_3$ substrates, while four-variant domain structures were observed in films grown on SrTiO$_3$-buffered substrates when the buffer layer is >2 nm thick.

DyScO$_3$ has an orthorhombic structure (space group *Pbnm*, lattice constants $a_0 = 5.440$ Å, $b_0 = 5.717$ Å, and $c_0 = 7.903$ Å)[21] which is the result of a cooperative oxygen octahedral rotation in an $a^-a^-c^+$ pattern (again in Glazer notation).[13] For a $(110)_O$ substrate, the orthorhombic unit cell can be related to a tilted pseudocubic (monoclinic) unit cell through the following equations: $a = \frac{c_0}{2} = 3.952$ Å, $b = c = \frac{\sqrt{a_0^2+b_0^2}}{2} = 3.947$ Å, $\alpha = 2\tan^{-1}\frac{a_0}{b_0} = 87.2°$, and $\beta = \gamma = 90°$. It is important to note that the difference between the two in-plane lattice parameters of the substrate is just 0.1%; while the difference between the angles α and β (γ) is over 3%. Unlike DyScO$_3$, bulk SrTiO$_3$ possesses a cubic structure without any octahedral rotations and lattice parameters $a = b = c = 3.905$ Å at room temperature. Therefore, nominally exact SrTiO$_3$ (001) should not possess any intrinsic anisotropy.

The BiFeO$_3$ films and SrTiO$_3$ buffer layers were grown by pulsed-laser deposition at 700 °C in an oxygen pressure of 100 mTorr and 2 mTorr, respectively. The BiFeO$_3$ film thickness was fixed at 50 nm for all samples. To rule out substrate vicinality effects,[22] all the films were grown on nominally exact DyScO$_3$ $(110)_O$ substrates with a miscut angle <0.1°. Detailed structural information was obtained using high-resolution X-ray diffraction (X'Pert MRD Pro, Panalytical) including $\theta - 2\theta$ scans and reciprocal space maps (RSMs). The surface morphology and domain structure were probed using atomic force microscopy (AFM) and piezoresponse force microscopy (PFM) (Asylum Research, Cypher).

A representative AFM topographic image [Fig. 1(b)] and $\theta - 2\theta$ XRD pattern [Fig. 1(c)] of a BiFeO$_3$ film grown on a 10-nm SrTiO$_3$-buffered DyScO$_3$ substrate reveal that the films are single-phase and epitaxial with a smooth surface. The presence of Laue oscillations further confirms that all films have good crystalline quality and smooth surfaces. Additional AFM studies of the as-grown SrTiO$_3$-buffered DyScO$_3$ substrates are also provided.[23]

Studies of the domain structure reveal uniform out-of-plane (vertical) PFM contrast suggesting that all domains have uniform out-of-plane polarization orientation.[23] The evolution of the in-plane domain structure with increasing SrTiO$_3$ buffered layer thicknesses is provided [Fig. 2]. In films grown directly on bare substrates [Fig. 2(a)], the domain patterns are dominated by one set of 71° stripe domains with domain walls aligned along $[001]_O$, leading to a

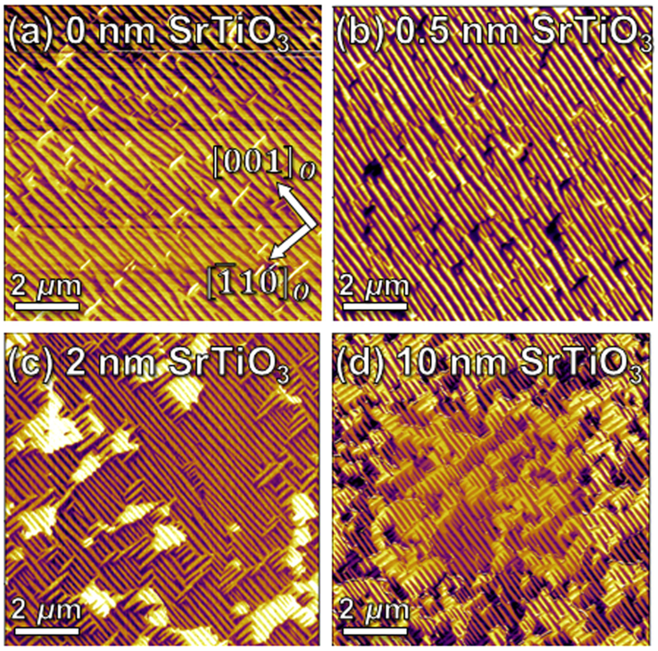

FIG. 2. In-plane PFM images of 50 nm BiFeO$_3$ films grown on DyScO$_3$ $(110)_O$ substrates with SrTiO$_3$ buffer layer thicknesses of (a) 0 nm, (b) 0.5 nm, (c) 2 nm, and (d) 10 nm.

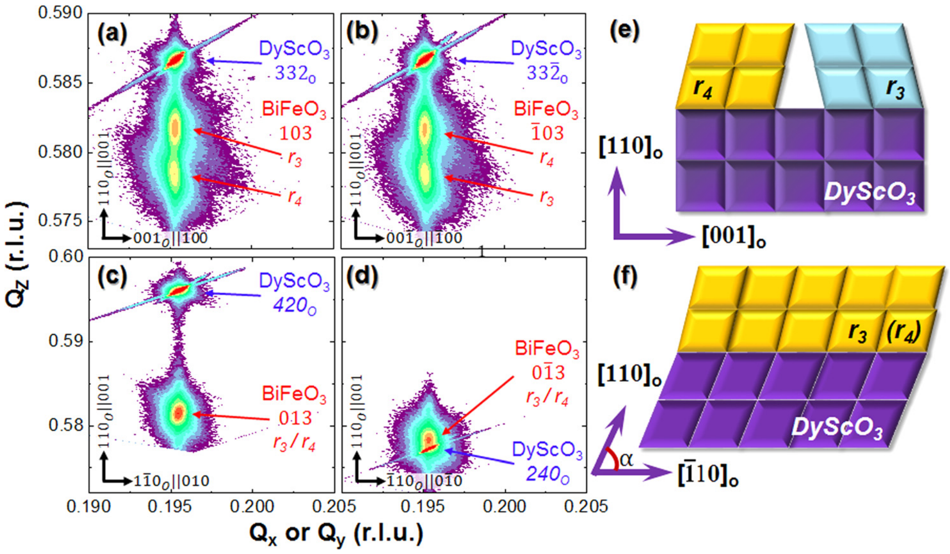

FIG. 3. RSMs of 50 nm $BiFeO_3$ film grown on bare $DyScO_3$ $(110)_O$ substrates about the $DyScO_3$ (pseudocubic $BiFeO_3$) (a) 332_O- (103-), (b) $33\bar{2}_O$- ($\bar{1}$03-), (c) 420_O- (013-), and (d) 240_O- (0$\bar{1}$3-) diffraction conditions. Schematic illustrations of the twinned domain structure along the (e) $[1\bar{1}0]_O$ and (f) $[001]_O$.

$BiFeO_3$ film with only two structural variants. Growth on a ~0.5 nm $SrTiO_3$ buffer layer [Fig. 2(b)] results, again, in primarily two-variant stripe domains. As the thickness of the $SrTiO_3$ buffer layer is increased to ~2 nm, however, a second, orthogonal set of 71° stripe domains with walls along $[1\bar{1}0]_O$ appears [Fig. 2(c)]. When the buffer layer thickness increases to 10 nm, the domain patterns are characterized by random combinations of two-variant stripe domains with all four structural variants present is essentially equal fractions [Fig. 2(d)], which is similar to the domain structure observed in films grown on nominal exact $SrTiO_3$ (001) substrates.[24]

To better understand the domain structure evolution, RSM studies were performed. RSM studies of $BiFeO_3$ films grown on bare $DyScO_3$ substrates about the $DyScO_3$ (pseudocubic $BiFeO_3$) 332_O- (103-) [Fig. 3(a)], $33\bar{2}_O$- ($\bar{1}$03-) [Fig. 3(b)], 420_O- (013-) [Fig. 3(c)], and 240_O- (0$\bar{1}$3-) [Fig. 3(d)] diffraction conditions all reveal that the in-plane lattice parameters of the film are coherently strained to the substrate. Peak splitting occurs in the $h0l$-diffraction condition, but not in the $0kl$-diffraction condition. The diffraction studies indicate that only two structural variants (r_3 and r_4, as defined in Fig. 1(a)) occur in the films grown on bare $DyScO_3$ substrates, consistent with the above PFM results and previous studies.[19] Because of the monoclinic nature of the substrate, the substrate 420_O-diffraction condition has a different position from the 240_O-diffraction condition. Likewise, the $BiFeO_3$ 013-diffraction condition also has a different position from the 0$\bar{1}$3-diffraction condition [Figs. 3(c) and 3(d)], indicating that the α angle of the $BiFeO_3$ pseudocubic unit cell deviates from 90°. A schematic illustration of the two domain motif, as viewed along the $[1\bar{1}0]_O$ [Fig. 3(e)] and $[001]_O$ [Fig. 3(f)], is provided for clarification. Because the substrate has a monoclinic distortion along the $[0\bar{1}1]$ ($[010]_O$), only two structural variants r_3 and r_4, which have a spontaneous shear distortion along $[\bar{1}\bar{1}1]$ and $[1\bar{1}1]$, respectively, could give rise to a net shear distortion along the monoclinic distortion of the substrate. Therefore, these two variants r_3 and r_4 are energetically favorable when the rhombohedral films are grown on $(110)_O$ substrates, in order to follow the substrate monoclinic distortion.

RSMs about the $DyScO_3$ (pseudocubic $BiFeO_3$) 332_O- (103-) and 420_O- (013-) diffraction conditions for $BiFeO_3$ films grown on a 10 nm $SrTiO_3$-buffered $DyScO_3$ substrate [Figs. 4(a) and 4(b), respectively] reveal that both the $BiFeO_3$ and $SrTiO_3$ films are coherently strained to the substrate; that is, both are under anisotropic in-plane strain. Additional RSMs for 60 nm thick $SrTiO_3$ films grown on $DyScO_3$ substrates also clearly reveal coherently strained films.[23] Unlike in the films grown directly on $DyScO_3$, however, clear peak splitting occurs in both $h0l$- and $0kl$-diffraction conditions, which typically occurs for $BiFeO_3$ films grown on $SrTiO_3$ substrates.[10,24] This is consistent with the above PFM results that show that all four structural variants are present in the films grown on the $SrTiO_3$-buffered substrate even though the film is still under anisotropic in-plane strain. Therefore, domain variant reduction in the films grown on $(110)_O$ substrates is likely not attributed to the

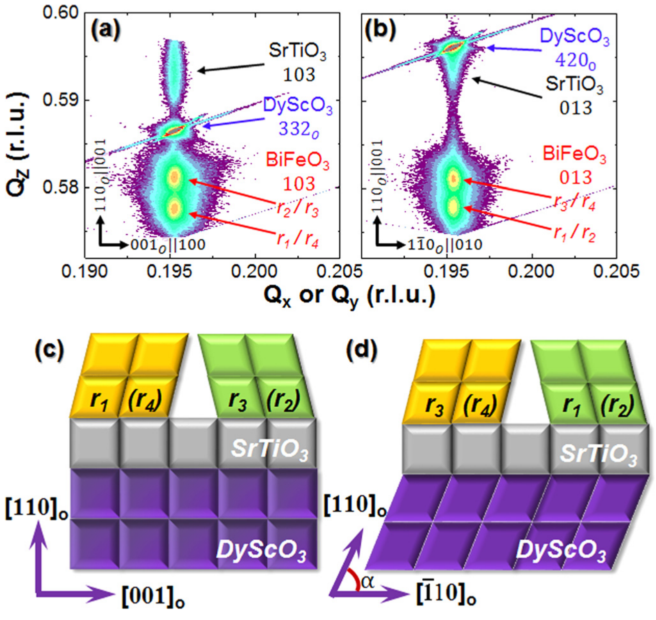

FIG. 4. RSMs of 50 nm $BiFeO_3$ film grown on 10-nm-thick $SrTiO_3$ buffered $DyScO_3$ $(110)_O$ substrate about the $DyScO_3$ (pseudocubic $BiFeO_3$) (a) 332_O- (103-) and (b) 420_O- (013-) diffraction conditions. Schematic illustrations of the twinned domain structure along the (c) $[1\bar{1}0]_O$ and (d) $[001]_O$.

in-plane anisotropic strain alone. Both theoretical and experimental studies have shown that, unlike lattice mismatch, the symmetry mismatch because of different oxygen octahedral tilting systems is normally relieved very rapidly (within only three to four unit cells from the interface).[25–28] In this context, as the thickness of the $SrTiO_3$ buffer layer exceeds 2 nm (or ~5 unit cells), the influence of the oxygen octahedral tilting from the $DyScO_3$ substrate is effectively diminished to a level where it can no longer impact the structure of the $SrTiO_3$ and it takes on a structure devoid of oxygen octahedral tilting and thus there is no monoclinic shear deformation in the topmost $SrTiO_3$ layers. This concept is schematically illustrated [Figs. 4(c) and 4(d)] and matches what is expected for films grown on cubic $SrTiO_3$ substrates directly where all four structural variants are present in the films when a relatively thick cubic buffer layer is inserted.

In conclusion, our experiments directly demonstrate that domain variant reduction in rhombohedral $BiFeO_3$ films grown on $(110)_O$ substrates cannot likely be attributed to anisotropic in-plane strain alone, but appears to be influenced by the presence of a monoclinic distortion, due to oxygen octahedral rotation, in the substrate. Such insights could be applied to other rhombohedral ferroic thin films, such as the ferromagnetic $La_{0.7}Sr_{0.3}MnO_3$ and ferroelectric $PbZr_{1-x}Ti_xO_3$ $(0.06 < x < 0.47)$, to manipulate the domain structures in these materials in a similar fashion. Our results also indicate that it is possible to tune the domain structure of ferroic thin films by engineering octahedral rotation coupling across interfaces. This is an intriguing observation since increasingly the community has been studying how 2-dimensional features, such as surfaces and interfaces, can produce effects that extend well into the bulk of the material. These observations offer yet another example of the power for heteroepitaxial interfaces in directing the evolution of materials.

Z.H.C. and L.W.M. acknowledge the support of the Army Research Office under Grant No. W911NF-10-1-0482, A.R.D. acknowledges the support of the National Science Foundation under Grant No. DMR-1149062, R.X. acknowledges the support of the National Science Foundation under Grant No. DMR-1124696, S.L. acknowledges support of the Air Force Office of Scientific Research under Grant No. MURI FA9550-12-1-0471. Experiments at UIUC were carried out, in part, in the Materials Research Laboratory Central Facilities.

[1] A. K. Tagantsev, L. E. Cross, and J. Fousek, *Ferroelectric Domains in Ferroelectric Crystals and Thin Films* (Springer, New York, 2010).

[2] N. Setter, D. Damjanovic, L. Eng, G. Fox, S. Gevorgian, S. Hong, A. Kingon, H. Kohlstedt, N. Y. Park, G. B. Stephenson, I. Stolitchnov, A. K. Taganstev, D. V. Taylor, T. Yamada, and S. Streiffer, J. Appl. Phys. **100**, 051606 (2006).

[3] M. Dawber, K. M. Rabe, and J. F. Scott, Rev. Mod. Phys. **77**, 1083 (2005).

[4] D. G. Schlom, L. Q. Chen, C. B. Eom, K. M. Rabe, S. K. Streiffer, and J. M. Triscone, Annu. Rev. Mater. Res. **37**, 589 (2007).

[5] J. M. Rondinelli, S. J. May, and J. W. Freeland, MRS Bull. **37**, 261 (2012).

[6] F. Sandiumenge, J. Santiso, L. Balcells, Z. Konstantinovic, J. Roqueta, A. Pomar, J. P. Espinós, and B. Martínez, Phys. Rev. Lett. **110**, 107206 (2013).

[7] A. Vailionis, H. Boschker, E. Houwman, G. Koster, G. Rijnders, and D. H. A. Blank, Appl. Phys. Lett. **95**, 152508 (2009).

[8] Y. H. Chu, Q. Zhan, L. W. Martin, M. P. Cruz, P. L. Yang, G. W. Pabst, F. Zavaliche, S. Y. Yang, J. X. Zhang, L. Q. Chen, D. G. Schlom, I. N. Lin, T. B. Wu, and R. Ramesh, Adv. Mater. **18**, 2307 (2006).

[9] C. M. Folkman, S. H. Baek, H. W. Jang, C. B. Eom, C. T. Nelson, X. Q. Pan, Y. L. Li, L. Q. Chen, A. Kumar, V. Gopalan, and S. K. Streiffer, Appl. Phys. Lett. **94**, 251911 (2009).

[10] F. Johann, A. Morelli, D. Biggemann, M. Arredondo, and I. Vrejoiu, Phys. Rev. B **84**, 094105 (2011).

[11] Z. H. Chen, Y. Qi, L. You, P. Yang, C. W. Huang, J. Wang, T. Sritharan, and L. Chen, Phys. Rev. B **88**, 054114 (2013).

[12] F. Kubel and H. Schmid, Acta Crystallogr., Sect. B: Struct. Sci. **46**, 698 (1990).

[13] A. Glazer, Acta Crystallogr., Sect. B: Struct. Crystallogr. Cryst. Chem. **28**, 3384 (1972).

[14] G. Y. Xu, H. Hiraka, G. Shirane, J. F. Li, J. L. Wang, and D. Viehland, Appl. Phys. Lett. **86**, 182905 (2005).

[15] S. K. Streiffer, C. B. Parker, A. E. Romanov, M. J. Lefevre, L. Zhao, J. S. Speck, W. Pompe, C. M. Foster, and G. R. Bai, J. Appl. Phys. **83**, 2742 (1998).

[16] F. Zavaliche, R. R. Das, D. M. Kim, C. B. Eom, S. Y. Yang, P. Shafer, and R. Ramesh, Appl. Phys. Lett. **87**, 252902 (2005).

[17] H. W. Jang, D. Ortiz, S. H. Baek, C. M. Folkman, R. R. Das, P. Shafer, Y. Chen, C. T. Nelson, X. Pan, R. Ramesh, and C. B. Eom, Adv. Mater. **21**, 817 (2009).

[18] J. Seidel, L. W. Martin, Q. He, Q. Zhan, Y. H. Chu, A. Rother, M. E. Hawkridge, P. Maksymovych, P. Yu, M. Gajek, N. Balke, S. V. Kalinin, S. Gemming, F. Wang, G. Catalan, J. F. Scott, N. A. Spaldin, J. Orenstein, and R. Ramesh, Nature Mater. **8**, 229 (2009).

[19] Y.-H. Chu, Q. He, C.-H. Yang, P. Yu, L. W. Martin, P. Shafer, and R. Ramesh, Nano Lett. **9**, 1726 (2009).

[20] J. X. Zhang, Y. L. Li, Y. Wang, Z. K. Liu, L. Q. Chen, Y. H. Chu, F. Zavaliche, and R. Ramesh, J. Appl. Phys. **101**, 114105 (2007).

[21] R. Uecker, B. Velickov, D. Klimm, R. Bertram, M. Bernhagen, M. Rabe, M. Albrecht, R. Fornari, and D. G. Schlom, J. Cryst. Growth **310**, 2649 (2008).

[22] Y. H. Chu, M. P. Cruz, C. H. Yang, L. W. Martin, P. L. Yang, J. X. Zhang, K. Lee, P. Yu, L. Q. Chen, and R. Ramesh, Adv. Mater. **19**, 2662 (2007).

[23] See supplementary material at http://dx.doi.org/10.1063/1.4875801 for a topographic image and x-ray reciprocal space mappings of single-layer $SrTiO_3$ films on $DyScO_3$ $(110)_O$ substrates and typical out-of-plane (vertical) PFM image of the $BiFeO_3$ films.

[24] Z. H. Chen, Z. Luo, Y. Qi, P. Yang, S. Wu, C. Huang, T. Wu, J. Wang, C. Gao, T. Sritharan, and L. Chen, Appl. Phys. Lett. **97**, 242903 (2010).

[25] J. He, A. Borisevich, S. V. Kalinin, S. J. Pennycook, and S. T. Pantelides, Phys. Rev. Lett. **105**, 227203 (2010).

[26] A. Y. Borisevich, H. J. Chang, M. Huijben, M. P. Oxley, S. Okamoto, M. K. Niranjan, J. D. Burton, E. Y. Tsymbal, Y. H. Chu, P. Yu, R. Ramesh, S. V. Kalinin, and S. J. Pennycook, Phys. Rev. Lett. **105**, 087204 (2010).

[27] R. Aso, D. Kan, Y. Shimakawa, and H. Kurata, Sci. Rep. **3**, 2214 (2013).

[28] C. L. Jia, S. B. Mi, M. Faley, U. Poppe, J. Schubert, and K. Urban, Phys. Rev. B **79**, 081405 (2009).